SEISMOLOGY ON PLUTO?! ANTIPODAL TERRAINS PRODUCED BY SPUTNIK PLANITIA-FORMING IMPACT. C. A. Denton[1], B. C. Johnson[1], A. M. Freed[1], and H. J. Melosh[1]. [1]Dept. of Earth, Atmospheric, and Planet. Sci., Purdue University, West Lafayette, IN 47907 (denton15@purdue.edu).

Introduction: Pluto's interior remains a mystery, including the composition of the core and the existence and extent of a subsurface ocean. Though typical seismological study is not possible on Pluto, the reaction of stress waves released from large impacts to a planet's interior structure can be used to probe the planet's interior – seismology by impact. Recent analysis of New Horizons data revealed extensive lineations antipodal to Sputnik Planitia (SP) [1], the 1200 x 2000 km elliptical impact basin on Pluto [2]. These resemble the "hilly and lineated" terrain antipodal to Caloris Basin on Mercury [3]; here, we propose a similar formation mechanism from seismic focusing of impact-generated stress waves. We simulate the formation of SP to determine if these terranes result from stress wave focusing at the basin's antipode [3-5], and how such focusing may have been influenced by Pluto's internal structure [3,5]. Our simulations reflect SP's updated dimensions [2], which require a larger impactor than previously considered [6]. Our numerical simulations consider variations in ocean thickness and core composition, as both are primary uncertainties in Pluto's internal structure that will exert significant control over wave propagation. We then compare predicted antipodal deformation to the geologic features observed to determine the most likely internal structure of Pluto.

Methods: Following [6], we use the iSALE shock physics code [7-9] to simulate a 300, 350, and 400-km diameter impactor striking a Pluto-like target at 2 km/s [10], with the same model setup [11-13]. A 400 km-impactor was found to produce the closest match to observed basin size and used as the fiducial model. We extend 2 km-resolution to all of Pluto to resolve antipodal deformation [i.e., 5]. In our simulations we vary preimpact ocean thickness (0, 50, 100, 150 km) and core composition (dunite [13], serpentine [14]) to determine which, if any, bulk interior structure yields the observed antipodal deformation. The combined ice shell/ocean thickness is held constant at 328 km [6]. Following [5], we infer resulting deformation through measurements of material velocity, total plastic strain, and displacement during and after stress wave arrival at the antipode.

Preliminary Results: In our fiducial model (D_{imp} = 400, t_{ocean} = 0, dunite core), the contrast in sound speeds between the ice shell (~3300 m/s) and core (~6500 m/s) causes the impact-induced stress wave to be transmitted quickly through the core and much more slowly through the overlying ice shell (reported sound speeds are calculated by iSALE using the equation of state). The temporal separation of the wave between materials produces separate arrivals at the antipode, as observed in strong peaks (>35 m/s) in material velocity (not to be confused with wave speed) at ~550 and ~800 s after impact. To assess structural deformation at the antipode, we quantify inward/outward displacement experienced by material in the region. Measurements of horizontal displacement after 5000 s (when the antipode is no longer accumulating plastic strain) indicate that greater than 2 km of displacement occurs in a near-surface zone extending 250 -300 km from the antipode, where material is largely carried inwards (Fig. 1a). This near-surface deformation zone is observed in all subsequent runs using a 400-km impactor (Figs. 1-2); decreasing impactor size reduces the width and magnitude of deformation.

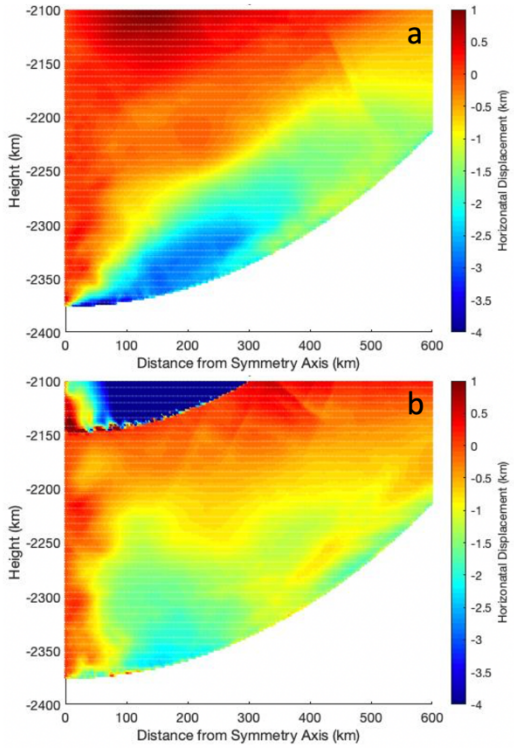

Figure 1. Tracer particles colored according to their displacement from the symmetry axis 5500 s after impact for a 400 km impactor and a dunite core. **a.** No ocean. **b.** 100-km ocean. The origin marks the point of impact (antipode at (0, -2376 km).

The addition of a liquid ocean between the ice shell and the core has an immediate weakening effect on the wave transmitted through the core to the antipode. The contrast in sound speeds between the core (~6500 m/s) and the ocean (~1900 m/s) far exceeds that of the core and the ice shell in the fiducial model, which reduces transmission of core waves to the antipode (Fig 1b). The

increase in reflection and decrease in transmission at the core-ocean interface reduces deformation prior to the arrival of the delayed wave in the ice shell, which decreases the overall amplitude of displacement at the antipode. Increasing ocean thickness further reduces core wave transmission, decreasing deformation; however, when the ocean is very thick (150 km) displacement amplitude is increased by the transmission of a much stronger wave through the thinner ice shell. In this scenario, the thinned ice shell acts as a waveguide.

When the dunite core is replaced with serpentine, the decrease in core sound speed to 5300 from 6500 m/s increases stress wave travel times and produces a delayed response in material velocity at the antipode (~680 and 1100 s for the core and ice shell wave arrivals, respectively). The reduced contrast in sound speeds between the core and the overlying ice shell facilitates greater transmission of energy to the antipode. As such, the region surrounding the antipode experiences higher magnitudes of lateral displacement (up to 14 km, Fig. 2a).

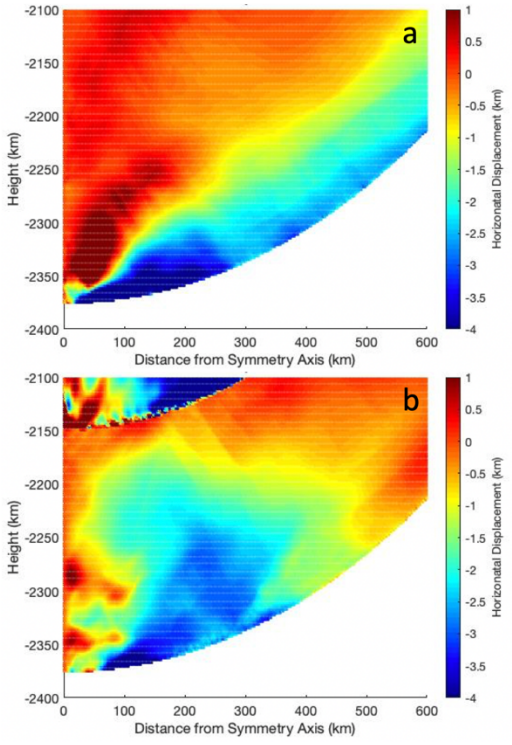

Figure 2. Same as Fig. 1, but with a serpentine core. **a.** No ocean. **b.** 100-km ocean.

The effects of the ocean in the dunite core models are also heightened by the reduced sound speed contrast with serpentine, which permits greater energy transmission and increases the magnitude of antipodal deformation for all ocean thicknesses tested (e.g., Fig. 2b). While sound speed contrasts at material interfaces appear to have the largest influence on wave travel patterns between compositional models, the magnitude of the arriving wave in the ice shell in serpentine core models is also amplified, despite a lack of interaction with the core. This response likely corresponds to focusing/defocusing of stress waves in transit [4-5].

Overall, a serpentinized core enhances deformation at the antipode relative to a dunite core for all ice shell/ocean structures tested, while the presence of an ocean decreases antipodal deformation relative to a Pluto composed solely of ice and rock. Currently, many of our simulations produce a significant zone of displacement that extends 600-1600 km in diameter centered on the antipode. This deformation zone is similar to the observed 800-1000 km-wide lineated terrain [1]. However, to determine which of these hypothesized internal structures may be most feasible, it is critical to resolve the expected strain in the near-surface to contrast with that expected from the lineations, which are tentatively interpreted as a graben system [1]. As such, we cannot yet resolve which of the initial suite of mechanical structures tested here may best correspond to the lineated terrain.

Conclusions: Initial analysis of impact simulations for development of antipodal terrain from the formation of the SP basin indicates that core composition and the presence/thickness of a subsurface ocean produce major differences in the magnitude and breadth of deformation at SP's antipode. Calculating strains near the antipode is the subject of ongoing work. We will use these strains to determine if the magnitude and regional extent of extensional strains in our simulations are consistent with observations of the lineated terrain. The sensitivity of displacement (Figs. 1-2) suggests these calculations will provide constraints on Pluto's interior structure, including the presence and thickness of an ocean and the hydration state of Pluto's core.

Acknowledgements: We gratefully acknowledge the developers of iSALE, including Gareth Collins, Kai Wünnemann, Dirk Elbeshausen, Tom Davison, and Boris Ivanov.

References: [1] Stern, S. A. et al. (2019) *arXiv:*1910.08833, astro-ph.EP. [2] Schenk, P. et al. (2018) *Icarus, 314,* 400-433. [3] Watts, A.M. et al. (1991) *Icarus,* 93, 159-168. [4] Schultz, P.H. and D.E. Gault (1974), *The Moon* 12, 159-177. [5] Bowling, T.J. et al. (2013) *JGR Planets* 118, 1-14. [6] Johnson, B.C. et al. (2016) *Geophys. Res. Lett, 43*, 10068-10077. [7] Amsden, A., et al. (1980) LANL Report, LA8095:101p. [8] Collins, G. S., et al. (2004) Meteoritics and Planetary Science, 39, 217-231. [9] Wünnemann, K., et al. (2006) Icarus, 180, 514-27. [10] Zahnle, K. et al. (2003) *Icarus, 231*, 394-406. [11] Bray, V.J. et al. (2014) *Icarus, 231*, 394-406. [12] Turtle, E.P. and E. Pierazzo (2001) *Science, 294*, 1326-1328. [13] Benz, W. et al. (1989) *Icarus, 81*, 113-131. [14] Brookshaw, L. (1988) *Tech. Rep. Working Paper Ser. SC-MC-9813.*